Direct optical fabrication of three-dimensional photonic crystals in a high refractive index $LiNbO_3$ crystal

Guangyong Zhou and Min Gu

Centre for Micro-Photonics and Centre for Ultrahigh-bandwidth Devices for Optical Systems, Faculty of Engineering and Industrial Sciences, Swinburne University of Technology, P. O. Box 218, Hawthorn, Victoria 3122, Australia

Received May 8, 2006; revised June 27, 2006; accepted July 6, 2006;
posted July 10, 2006 (Doc. ID 70700); published August 25, 2006

Direct optical fabrication of 3D photonic crystals in a high refractive index $LiNbO_3$ crystal by using the femtosecond laser-induced microexplosion method is investigated. The focal distortion, caused by the refractive index mismatch-induced spherical aberration, can be significantly reduced by using a so-called threshold fabrication method. As a result, 3D fcc photonic crystals are fabricated by stacking quasi-spherical voids layer by layer. Photonic stopgaps with suppression rates of up to 30% in the transmission spectra are observed. The angle dependence of the stopgaps is also revealed. © 2006 Optical Society of America

OCIS codes: 220.4000, 080.1010, 160.3730, 160.4670, 140.3390.

Ultrafast laser-induced microexplosions have been proved to be an efficient method to fabricate 2D and 3D photonic crystals in transparent solid materials with a relatively low refractive index, such as polymers,[1–6] silica, and glasses.[7] The refractive index of those materials is ~1.5 and is similar to that of the immersion oil (1.52). Therefore the refractive index mismatch-induced spherical aberration is not strong and can normally be neglected in most microfabrication processes. However, the low refractive index does not make those materials ideal for photonic crystal fabrication. For photonic crystals, the higher the refractive index contrast, the easier it is to open large or complete bandgaps. One needs to fabricate photonic structures in high refractive index materials.

Lithium niobate ($LiNbO_3$) is a well-known nonlinear crystal with a high refractive index of 2.2 and a large transparent range of 0.5–5 μm, making it an ideal candidate material for photonic crystals.[8,9] Furthermore, nonlinear effects and therefore functional devices are expected from $LiNbO_3$-based photonic crystals because of their strong nonlinear effects, such as the Kerr effect.[10–12] 2D hexagonal photonic crystals with a thickness of 1.5 μm have been fabricated by using a focused ion-beam etching method, but it is very difficult to fabricate thick 3D photonic crystals.[13] Our previous results have shown that micrometer-sized voids can be generated deep inside $LiNbO_3$ by using the femtosecond laser-induced microexplosion method.[14] However, the large refractive index mismatch between $LiNbO_3$ and the immersion medium of the objective will introduce a very strong spherical aberration effect at the focalus region.[15,16] To fabricate photonic crystals in $LiNbO_3$, one needs to understand the spherical aberration.[15] In this Letter, we first investigate the effect of spherical aberration and then the fabrication of 3D photonic crystals, for the first time to the best of our knowledge by using the femtosecond laser-induced microexplosion method. The photonic bandgap properties are also investigated.

When a light beam is focused by a high NA oil immersion objective into a slab of $LiNbO_3$, the diffraction pattern at the focal region is distorted compared with the diffraction-limited pattern in a refractive

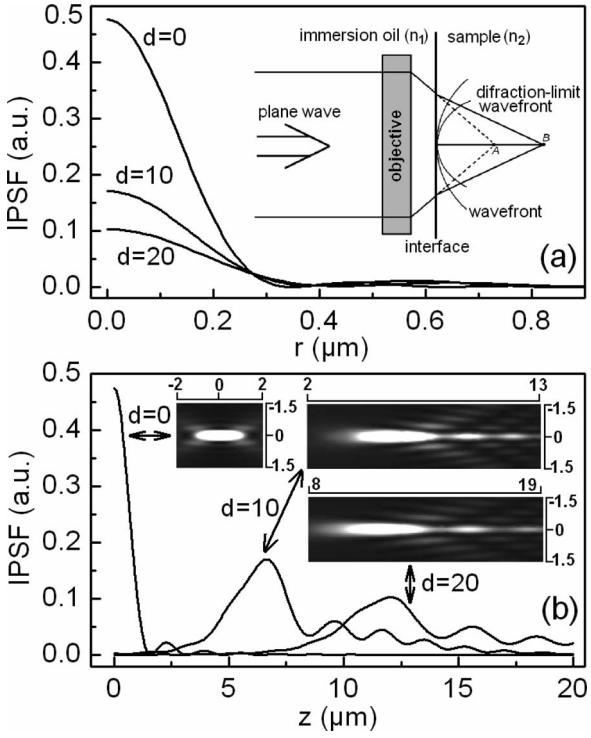

Fig. 1. (a) Transverse and (b) axial cross sections of the 3D IPSF at different depths in the $LiNbO_3$ slab for a 1.4 NA oil immersion objective. The inset in (a) shows the principle of refractive index mismatch-induced spherical aberration. The insets in (b) show the intensity distribution in the focus region at different depths.

0146-9592/06/182783-3/$15.00

index-matched medium, as shown in the inset in Fig. 1(a). Figure 1(a) shows the transverse cross section of the 3D intensity point spread function (IPSF), calculated by using the diffraction theory,[15,16] when a plane-wave light is focused into the $LiNbO_3$ slab through an NA 1.4 oil immersion objective. An average refractive index of 2.2 for $LiNbO_3$ is used. When the light is focused on the surface, the diffraction-limit focus has the highest peak intensity and the narrowest spot size. When the light is focused into the crystal, the peak intensity drops dramatically, as shown in Fig. 1(a). In the meantime, the focus region becomes broader slightly in the transverse direction. Figure 1(b) shows the axial cross section of the 3D IPSF. Apart from the intensity drop and focus broadening as seen in the transverse direction, there is a clear focus shift and several obvious sidelobes. The focus shifts as a function of the diffraction-limited focus depth is shown in Fig. 2, where an almost linear dependence is observed. As the origin of the coordinate located at the diffraction-limit focus, the slope of this curve, ~0.6, means that the real focus in the crystal moves 1.6 μm as the objective or the diffraction-limited focus moves 1 μm. From the intensity distribution of the focal region in the inset in Fig. 1(b), one can clearly see the distortion of the focus and its sidelobes along the axial direction. The lower-order sidelobes may produce unwanted effects in experiments if the laser power is so high that the intensity of the sidelobe is higher than the threshold. If one can choose the laser power properly, making the main peak of the IPSF slightly above the threshold and all the sidelobes below the threshold, the sidelobes can be removed.

To confirm the linear dependence and the feasibility of the threshold fabrication method, we measured the side view of the voids that represents the IPSF at the focus region by using a confocal microscope (Fluoview, Olympus, Japan). In this work, a standard microfabrication setup was used.[14] A 750 nm irradiation with pulse duration of 100 fs coming from a femtosecond oscillator with a repetition rate of 82 MHz (Tsunami, Spectra-Physics, Mountain View, California) was tightly focused into the crystal through an Olympus 60×, NA 1.4 oil immersion objective. The crystal was affixed to a computer-controlled piezoelectric scanning stage (PI, Germany). 0.01% iron-doped $LiNbO_3$ was used because it has a larger Kerr effect[11,12] and a lower fabrication threshold than the pure one.[14] The crystal was cut into 2mm × 2mm × 10mm pieces with four large faces polished. To measure the side view of the fabricated voids, the sample was rotated 90° after fabrication. Figure 3(a) shows the typical shape of the voids when the laser power is much higher than the threshold. Clearly, the sidelobes can also generate voids when the laser power is high enough. The dumbbell-shaped and exclamatory-mark-shaped voids in Figs. 3(b) and 3(c) show the effect of the first and the first two sidelobes, respectively. Reducing the laser power to the condition that only the main peak is slightly above the threshold results in quasi-spherical voids, as shown in Fig. 3(d). Figure 3(d) also shows the voids fabricated at the depths from 43 to 67 μm, which gives the dependence of the focal shift on the depth [see the solid diamonds (♦) in Fig. 2]. The slope of the experimental curve of 0.62 agrees well with that of the calculated one. It should be pointed out that the images shown in Fig. 3 were obtained in a transmission mode. Thus they do not exhibit the weak change in refractive index caused by the photorefractive effect.

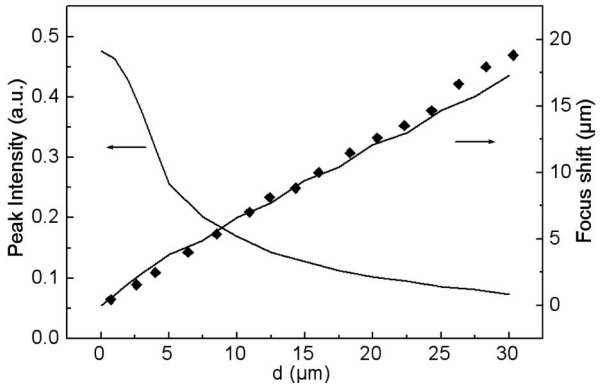

Fig. 2. Peak intensity of the IPSF and the calculated focus shift as a function of the focus depth in the $LiNbO_3$ slab. The solid diamonds (♦) denote the experimental focus shifts. The objective is the same as in Fig. 1.

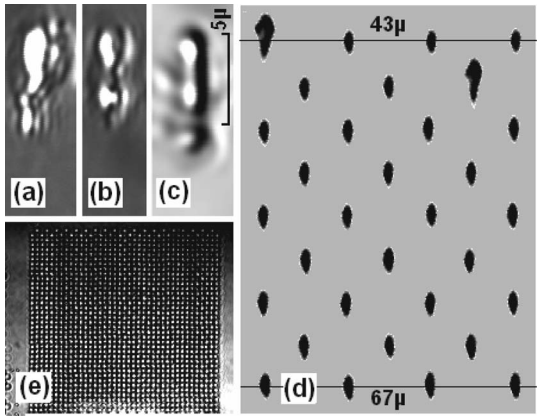

Fig. 3. (a)–(c) Side-view confocal transmission images of voids fabricated in the $LiNbO_3$ slab with a power far above the threshold. (d) Side-view confocal transmission image of voids at different depths fabricated near the threshold with a depth difference of the diffraction-limit focus between adjacent rows of 2 μm. (e) Confocal transmission image of a 16-layer fcc structure with a lattice constant of 4.5 μm.

Based on the understanding of focus shifts under the threshold condition, we have fabricated 3D fcc photonic crystals in the $LiNbO_3$ slab. The 16-1ayer structures were stacked with quasi-spherical voids layer by layer with the deepest layer fabricated first. During the fabrication process, the laser power needs to be adjusted to meet the threshold for each layer, which is determined by Fig. 2. Figure 3(e) shows the confocal transmission image of a structure with a lattice constant of 4.5 μm. The photonic properties were measured by using a Fourier transform infrared spectrometer with a NA 0.65 reflective objective (Thermo Nicolet, Madison, Wis.). Figure 4 shows the transmission spectra of the fabricated structures at

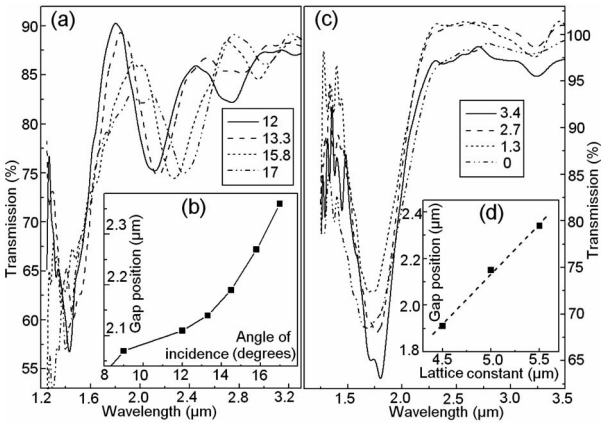

Fig. 4. (a) Transmittance spectra of the 16-layer fcc structure with $a=4.5\ \mu$m for the angle of incidence from 12° to 17°. (b) Dependence of the gap position on the angle of incidence. (c) Transmittance spectra of the 16-layer fcc structure with $a=4.5\ \mu$m for the angle of incidence from 0° to 3.4°. (d) Dependence of the gap position on the lattice constant.

various angles of incidence measured by using the angle-resolved method.[6] In Fig. 4(a), one can see that there is an obvious stopgap at around 2.2 μm with a suppression rate of ~15%. The position of the stopgap is dependent on the angle of incidence, as shown in Fig. 4(b). By increasing the angle of incidence from 9° to 17°, the central position of the gap shifts from 2.07 to 2.36 μm. As shown in Fig. 4(c), the suppression rate of the stopgap increases dramatically to more than 30% at small angles of incidence (<4°). Figure 4(d) shows the gap position of photonic crystals with a lattice constant of 4.5, 5, and 5.5 μm at an angle of incidence of ~5°. As expected, a linear relationship was observed.

It should be pointed out that the bandgap in $LiNbO_3$ is not deep enough. One main reason is that the fabricated voids are still not uniform. Although the effect of the sidelobes can be removed by using this threshold fabrication method, the strong spherical aberration effect is not completely removed, and it is difficult to fabricate uniform voids at different depths. Another reason is that the surface of the voids is not smooth. The femtosecond laser-induced high pressure may introduce a structure change of $LiNbO_3$ around the voids.[17] To further improve the fabrication quality, it is necessary to use the phase compensation technique to remove the effect of the spherical aberration caused by the large refractive index mismatching.[18,19]

In summary, based on the theoretic prediction of the focal shift and distortion, we have developed the focal-shift-threshold method. As such, we have successfully fabricated 3D photonic crystals in a high refractive index $LiNbO_3$ crystal by using the femtosecond laser-induced microexplosion method. Photonic bandgaps with suppression rates of 30% in the transmission spectra have been observed. Although the quality of the photonic crystals needs to be improved, this technique opens a door to direct optical fabrication of 3D nonlinear photonic crystals in a high refractive index $LiNbO_3$ crystal.

The work is supported by an Australian Research Council (ARC) Discovery project and ARC Centres of Excellence Program. The Centre for Ultrahigh-bandwidth Devices for Optical Systems (CUDOS) is an ARC Centre of Excellence. G. Zhou's e-mail address is gzhou@swin.edu.au. M. Gu's e-mail address is mgu@swin.edu.au.

References

1. E. N. Glezer and E. Mazur, Appl. Phys. Lett. **71**, 882 (1997).
2. H.-B. Sun, Y. Xu, S. Juodkazis, K. Sun, M. Watanabe, S. Matsuo, H. Misawa, and J. Nishii, Opt. Lett. **26**, 325 (2001).
3. D. Day and M. Gu, Appl. Phys. Lett. **80**, 2404 (2002).
4. M. J. Ventura, M. Straub, and M. Gu, Appl. Phys. Lett. **82**, 1649 (2003).
5. G. Zhou, M. J. Ventura, M. Straub, and M. Gu, Appl. Phys. Lett. **84**, 4415 (2004).
6. G. Zhou, M. J. Ventura, M. R. Vanner, and M. Gu, Appl. Phys. Lett. **86**, 011108 (2005).
7. H.-B. Sun, Y. Xu, K. Sun, S. Juodkazis, M. Watanabe, S. Matsuo, H. Misawa, and J. Nishii, Mater. Res. Soc. Symp. Proc. **605**, 85 (2000).
8. T. Kartaloglu, Z. G. Figen, and O. Aytur, J. Opt. Soc. Am. B **20**, 343 (2003).
9. B. Andreas, K. Peithmann, K. Buse, and K. Maier, Appl. Phys. Lett. **84**, 3813 (2004).
10. K. Noguchi, H. Myazawa, and O. Mitomi, Electron. Lett. **34**, 661 (1998).
11. H. T. Hsieh, D. Psaltis, O. Beyer, D. Maxein, C. K. Schmising, K. Buse, and B. Sturman, Opt. Lett. **30**, 2233 (2005).
12. O. Beyer, I. Breunig, F. Kalkum, and K. Buse, Appl. Phys. Lett. **88**, 051120 (2006).
13. M. Roussey, M. P. Bernal, N. Courjal, and F. I. Baida, Appl. Phys. Lett. **87**, 241101 (2005).
14. G. Zhou and M. Gu, Appl. Phys. Lett. **87**, 241107 (2005).
15. M. Gu, *Advanced Optical Imaging Theory* (Springer, 2000).
16. D. Day and M. Gu, Appl. Opt. **37**, 6299 (1998).
17. S. Juodkazis, N. Nishimura, S. Tanaka, H. Misawa, E. G. Gamaly, B. Luther-Davies, L. Hallo, P. Nicolai, and V. T. Tikhonchuk, Phys. Rev. Lett. **96**, 166101 (2006).
18. M. J. Booth and T. Wilson, J. Biomed. Opt. **6**, 266 (2001).
19. M. J. Booth, M. Schwertner, T. Wilson, M. Nakano, Y. Kawata, M. Nakabayashi, and S. Miyata, Appl. Phys. Lett. **88**, 031109 (2006).